TiO2 Thin Nanosheets Enhance to the Antimicrobial Activity two Gram Positive Bacteria and two Gram Negative Bacteria

Shinde S.A.[1], J.R. Kote[2]
[1]*Department of Physics, Sharadchandra ACS College Naigaon. Dist-Nanded, MS*
[2]*School of Life science, Department of Botany SRTMU Nanded, MS*

INTRODUCTION

Envisaging the role of TiO_2 in theranautics and biomedicine it is immensely important to evaluate its antimicrobial activity. Hence in this study TiO_2 thin nanosheets (TiO_2) were synthesized using wet chemical solution method at a very low refluxing temperature (90 oC) and short time (60 min). Scanning electron microscopy of the grown structure revealed micro flowers (2~3 μm) composed of thin sheets petals (60~80 nm). The thickness of each individual grown sheet varies from 10~20 nm. Antimicrobial activities of TiO_2 against two Gram positive bacteria (*Micrococcus luteus*, and *Staphylococcus aureus*), and two Gram negative bacteria (*Escherichia coli* and *Pseudomonas aeruginosa*) were determined. A 98% and 65% growth inhibition of *M. luteus and S. aureus* respectively, was observed with 500 μg/ml of CoO-TNs compared to 39 and 34% growth inhibition of E. coli and *P. aeruginosa*, respectively with the same concentration of TiO_2. Hence, synthesized TiO_2 exhibited antimicrobial activity against Gram negative bacteria and an invariably higher activity against tested Gram-positive bacteria. Therefore, synthesized TiO_2 are less prone to microbial infections.

The conversion of sunlight into electricity is a clean, abundant, and renewable energy source. The efficiency of conventional solar cells made from inorganic materials reached up to 24% [1], using very expensive materials of high purity and energy intensive processing techniques. New ways of manufacturing solar cells that can scale up to large volumes and low cost are required. A broad range of solar cell technologies are currently being developed, including dye-sensitized nanocrystalline photo-electrochemical solar cells, polymer/fullerene bulk hetero-junctions, small molecule thin films and organic–inorganic hybrid devices.

As discussed earlier, dye-sensitized solar cells (DSSC) have been investigated as one of the potential candidates for next-generation solar cells due to the high power-conversion efficiency and low cost compared with *p-n* junction photovoltaic devices [2, 3]. DSSC have been intensively studied [4, 5] for the possible replacement of fossil fuels as energy source since solar energy is considered inexhaustible compared with other energy forms. The DSSC have the advantages of simple fabrication, low cost, and large areas. Recent research has indicated that the photoelectric conversion efficiency over 11% can be achieved [6, 7], but this is still lower than that of conventional silicon solar cells. Accordingly, various investigations have been undertaken to enhance the efficiency of DSSC, in particular, the use of a compact layer between the transparent conductive oxides (TCOs) and nano-porous TiO_2 has been actively studied [8,9]. The compact layer can be fabricated by various methods such as sputter deposition [10], dip-coating [11], chemical vapor deposition [12], and spray pyrolysis [13]. The power generation in DSSC is based on photoexcitation of dye molecules, which injects the photoelectrons into a TiO_2 film that leads the electrons toward the external circuit [14]. TiO_2 nanotubes can serve as the material of photoelectrode because of their large surface area; their porous structure facilitates electrolyte diffusion. Therefore, a photoelectrode fabricated from TiO_2 nanotubes can smooth the transmission path for photoelectrons and reduce the possibility of the recombination of electrons and holes generated from photoelectrons with the electrolyte [15, 16]. In addition, TiO_2 particles fabricated by different methods can increase the length

of the path, along which photons pass through light-scattering properties if TiO_2 particles with good properties of optical transmittance and scattering properties are used [17]. A mesoporous nanocrystalline structure (TiO_2 nanoparticles constituting film) [18] decreases the back-reaction sites on FTO and yields corresponding improvement of the performance of DSSC. The working principle of this coating as mostly reported [21], is to improve electron transport across the TiO_2 mesoporous layer by enhancing the connectivity among TiO_2 particles.

The interfacial contact between chemically grown TiO_2 nanostructures and conducting substrate consists of various defects and lattice mismatch which can hinder an easy transportation of excited electrons by producing low current density and power conversion efficiency.

In the present study rutile TiO_2 were synthesized using a cost-effective and simple wet chemical, commonly preferred chemical bath deposition, method. In, glass, containers, and effect of container environment on the structural, morphological and optical properties is studied. It is found that the rate of reaction was glass container environments. Reaction was not operated in ferrous container. This can be explained on materials oxidation point of view used as a container environment. Charge transport kinetics was systematically explored to understand variation in performance for TiO_2 nanostructures.

CHEMICAL BATH DEPOSITION

Unlike the physical methods of preparation of thin films involving evaporation or ejection of material from a source, chemical methods of thin film deposition entail a definite chemical reaction. Chemical methods for film deposition in general use simpler equipment and are more economical than physical approaches. Moreover, chemical methods do not require high vacuum and can be carried out at lower temperatures. Chemical bath deposition (CBD) is simple & low-cost method that produces uniform adherent & reproducible large area thin films for PV related applications [22].

In chemical bath deposition, a complexing agent is used to bind the metallic ions to avoid the homogeneous precipitation of the corresponding compound. Formation of complex ion is essential to control the rate of the reaction and to avoid the immediate precipitation of the compound in the solution. The metal complex hydrolyses slowly to generate the positive ions in the solution. The solution containing the metal complexes can be mixed with the solution which produces the negative ion by hydrolyses. The deposition of the compound occurs when the ionic product exceeds the solubility product of the compound to be deposited. Either homogeneous or heterogeneous deposition can occur. The homogeneous process is the faster one resulting in the adsorption of powdery particles on the substrate due to the bulk precipitation. So, the formation of metal complexes is essential to minimize the homogeneous process. In the heterogeneous process, due to the slow release of the ion by metal complexes the preferential absorption of ions will take place leading to the uniform nucleation & growth of the thin film onto give substrate surface.

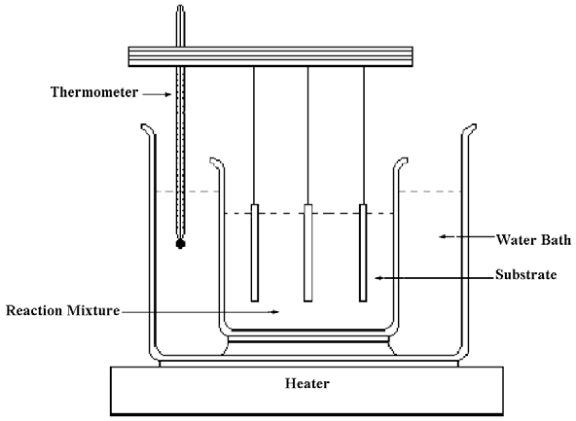

Figure 1.2 Set up for Chemical bath deposition method

The main disadvantage of the chemical bath deposition method is the wastage of the material due to the deposition on the walls of the container and precipitation into the solution. Preparation of the films with a definite geometric pattern on the substrate is difficult because perfect masking is not possible. The quality of the film deposited depends on the bath parameters like temperature, time of deposition, concentration of the reactants and the pH of the chemical bath. The experimental set up for the chemical bath deposition is shown in figure 3.1. Although chemical bath deposition has been used as a technique for preparing films since 1960, utilization of CBD semiconductors in photovoltaic devices started only since 1990 by integrating CdS buffer layer over sputtered ZnO films [23]. A number of review articles

discussing the status and applications of CBD have been appeared in the literature [24, 25]. In this thesis work we synthesized TiO_2 nanostructors in by CBD method in different container environments. Container environments including stainless-steel, glass, plastic, silver and copper etc were used.

EXPERIMENTAL DETAILS

All chemicals used for synthesizing TiO_2 nanostructures were of analytical grade taken from Merck and utilized without any further purification. Solution of $TiCl_4$ was firstly reduced to 1 M solution in 20% HCl by adding the calculated ml of HCl, triply distilled water and $TiCl_4$ solution. This mixture was then kept at 373 K for 30 minutes; the yellow color of solution was turned to colorless. This prepared solution was used as a stock solution. Fluorine-tin-oxide substrates purchased from SAMSUNG electronics were used on account of their good stability at high temperature and transparency. FTO substrates were washed with acetone in an ultrasonic bath at room temperature for 30 min. in $TiCl_4$ solution 0.1 M thiourea was added slowly with stirring while Antimicrobial activity of TiO_2

A attentiveness dependent growth inhibition of all four tested strains was observed with TiO_2. Growth of *Streptococcus bovis* a Gram-positive bacterium was inhibited by 1, 15, 20, 23, 27 and 34% with 25, 50, 100, 200, 300 and 500 µg/ml of TiO_2, respectively (Fig. 5a). While the growth of *Bacillus subtilis* decreased by 4, 2, 7, 20, 30 and 39% with 25, 50, 100, 200, 300 and 500 µg/mL of TiO_2, respectively (Fig. 5b). The growth of Gram positive bacteria *M. luteus* was inhibited by 25, 47, 76, 98, 99 and 98% with 25, 50, 100, 200, 300 and 500 µg/ml of TiO_2, respectively (Fig. 6a) and a growth inhibition of 13, 53, 58, 59, 62 and 65% was observed for another Gram positive bacteria *S. aureus* with 25, 50, 100, 200, 300 and 500 µg/mL of TiO_2, respectively (Fig. 6b). It is clear from the comparison of (Fig. 5) and (Fig. 6) that TiO_2 is more effective against Gram positive bacteria tested in this study. In another similar study the antimicrobial activity of TiO_2 with as average size of 9.13 nm against Bacillus subtilis (Gram positive) and *Salmonella typhimurium* (Gram negative) was tested, and interestingly the antimicrobial activity was observed only against *Bacillus subtilis* [20]. The reasons for selective activity of TiO_2 and its mode of action against bacteria is a matter for future studies.

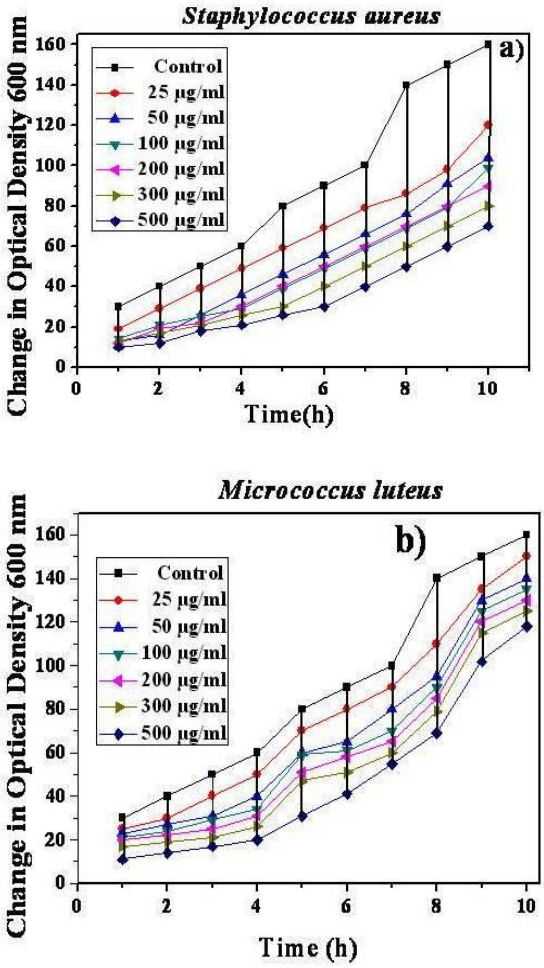

Fig.2 Growth prevention of Gram-positive bacteria a) Staphylococcus aureus B) Micrococcus luteus with various concentration of TiO_2.Error bars standard derivation and asterisk indicate significant values ($p < 0.05$)

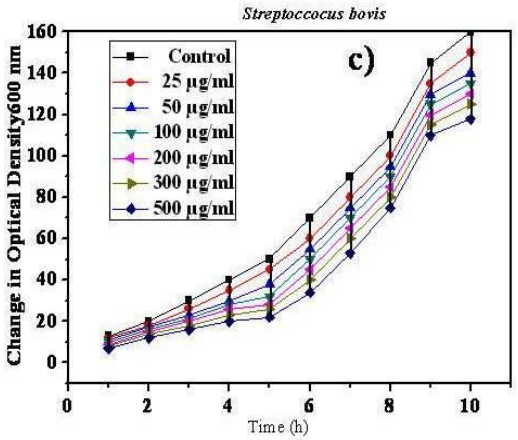

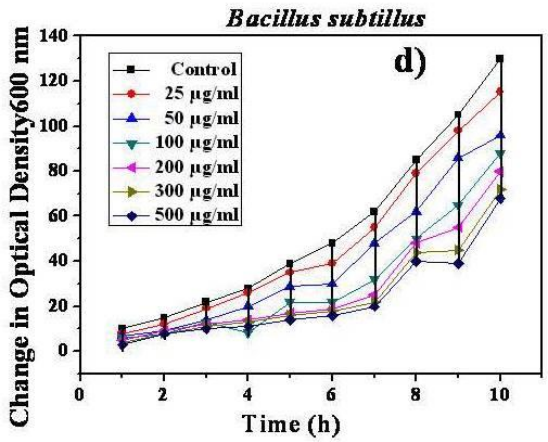

Fig.3 Growth inhibition of Gram-positive bacteria c) *Streptococcus bovis* d) *Micrococcus luteus* with various concentration of TiO_2. Error bars standard derivation and asterisk indicate significant values ($p < 0.05$).

CHARACTERIZATION DETAILS

Structural elucidation

The XRD spectra of the TiO_2 films of different nanostructures obtained from different container environments is presented in figure 3.2. There was no significant change in XRD behavior of TiO_2. Obtained peaks were analyzed and confirmed with JCPDS data file no. 16-0617. No peaks belong to any other phases such as brookite and anatase were detected, clearly indicating that the sample was of high purity and with a single phase i.e. rutile.

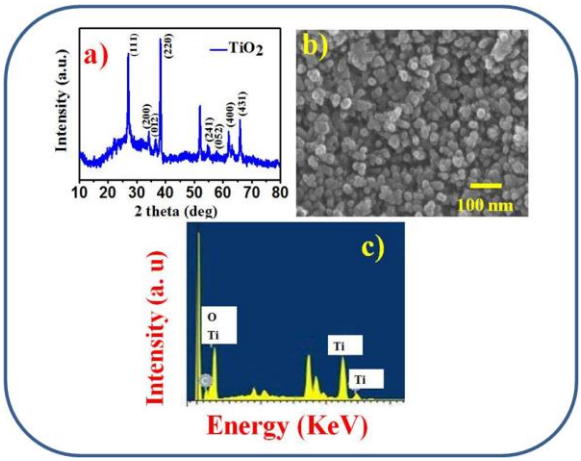

Figure 3.2: a) XRD plot of the TiO_2, b) SEM, c) EDX

All the graphs were with identical peaks and did not revealed substantial variation. The peaks obtained have the characteristic diffraction peaks corresponding to (111), (200), (012), (220),(241), (400) and (431) planes of rutile TiO_2 and calculated average grain sizes for TiO_2 were about 23.66 nm.

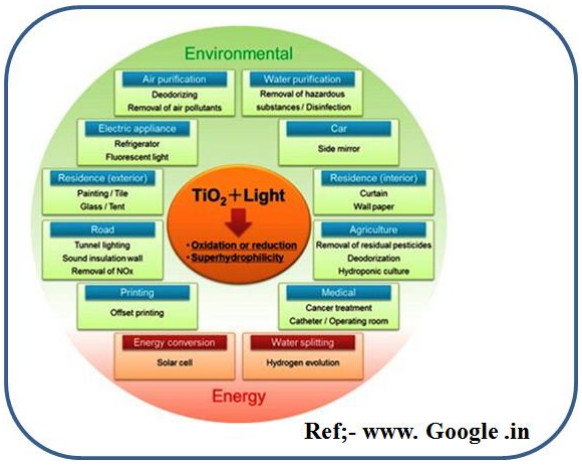

MORPHOLOGICAL EVOLUTION

Surface morphological study of TiO_2 nanostructures was carried out by the field emission scanning electron microscopy (SEM). From the FE-SEM images it was clearly observed that although nanoparticles are prepared by same synthesis method but there was variation in morphology due to use of different physical environmental conditions. Tilted nano crystallites were connected to each other at the base and then grow vertically. Few crystallites were elongated and separated from one another.

SAED and HR-TEM analysis

Figure 3.4 (a) shows the SAED pattern image of TiO_2 nano rice morphology were obtained. A set of rings instead of spots due to random orientation of the nano crystallites inside the nanoplates were seen. Interplanar spacing differences were 3.24, 2.51 and 1. 68 Å correspond to ruitle again supporting the fact that deposited TiO_2 was of rutile in phase, consistent to XRD results.

ATEM images TiO_2 film in glass container shown in Figure 3.4. The bar system estimated grain size (15 nm) for TiO_2 thin films are in good agreement with the mean diameter from the TEM image, indicating the nanocrystalline nature of the particles. TiO_2 films are composed of closely and loosely packed nanoparticles of about 15 nm diameter, which is remarkable because nanostructured titanium dioxide exhibits important properties and is now the subject of intensive investigation. We hope that the measurements and

results provided here will be of use to theorists interested in testing the models for quantum-confined structures.

RAMAN SPECTROSCOPY

Figure 3.5 (a) confirmed O $1s_{1/2}$ peak with binding energy of 530.02 eV, which can be assigned to the O $1s_{1/2}$ of TiO_2. The Ti $2p_{1/2}$ and Ti $2p_{3/2}$ peaks were obtained at 460.53 and 465.92 eV, respectively, which were closely match to that reported elsewhere [26]. The obtained elemental Ti $2p_{1/2}$ and Ti $2p_{3/2}$ peaks shifted toward binding energies higher than 455 and 461 eV, while the obtained O 1s1/2 peak shifted toward a low binding energy (530.02 eV) when compared with pure Ti [27], again supporting the formation of TiO_2 in contrast to metallic Ti. A representative Ramam spectrum obtained from the room temperature Raman spectroscopy carried out on these TiO_2 spongy-type spheres, obtained from the glass container, is shown in Figure 3.5 (b) wherein, three major peaks at 238, 240 and 609 cm^{-1} corresponds to B_{1g}, E_g and A_{1g} as active modes can be identified. These peak positions match closely to references values reported by Begun et al [28] (235, 443 and 610 cm^{-1}), Ma et al [29] (450 and 610 cm^{-1}) and Amin at al [30] (238, 444 and 609) for rutile TiO_2, indicating the as-synthesized TiO_2 nanoplates were of the rutile form. Raman peaks for anatase phase TiO_2 [21] (515 and 640 cm^{-1}) were absent in acquired Raman spectra again confirming anatase phase-free TiO_2 deposition.

CONCLUSION

Based on the results presented in this manuscript it is concluded that controlling reaction parameter is crucial for the synthesis of TiO_2 Thin nanosheets in an aqueous media. Characterization of synthesized nanostructures using XRD SAED, HR-TEM and SEM analysis shows that grown structures of TiO_2 exhibit a SAED pattern image of TiO2 nano morphology were obtained. (100 nm), our study found that the grown TiO2 shows excellent antimicrobial activity against four Gram positive bacteria and behave as a new antimicrobial agent at 500 μg/ml. Rutile TiO_2, indicating the as-synthesized TiO_2 nanoplates were of the rutile form. The detailed mechanism of the TiO_2 antimicrobial activity warrants further studies.

REFERENCES

[1] M. Green. (2001) Third generation photovoltaics: Ultra-high conversion efficiency at low cost Progr. Photovolt. 251:9-123.

[2] B. O'Regan, M. Grätzel. (1991) A low-cost, high-efficiency solar cell based on dye-sensitized colloidal TiO_2 films. Nature. 353:737–740

[3] M. Grätzel. (2005) Solar Energy Conversion by Dye-Sensitized Photovoltaic Cells. Inorg. Chem. 44 (20), 6841–6851

[4] M. Grätzel. (2001) Photo electrochemical cells *Nature*, 414. 338–344.

[5] M. Grätzel (2004) Conversion of Sunlight to Electric Power by Nanocrystalline Dye Sensitized Solar Cells. J. Photochem. Photobiol. A: Chem., 164.3-14.

[6] H.Yu, S. Zhang, H. Zhao,G. Will, P. Liu. (2009) An efficient and low-cost TiO2 compact layer for performance Electrochim. Acta, 54 (4), 1319–1324.

[7] J. Shi, J. Liang, S. Peng, W. Xu, J. Pei, J. Chen. Ni1−x Pt x (x=0–0.08) (2009) films as the photocathode of dye-sensitized solar cells with high efficiency Solid State Sci.,11 433.

[8] J. Xia, N. Masaki, K. Jiang, S. Yanagida. (2006) The Photovoltage-Determining Mechanism in Dye-Sensitized Solar Cells. J. Phys. Chem. B, 104 (1) 6–10.

[9] W.Y. Gan, S.W.Lam, K.Chiang, R.A mal, H. Zhao, M. P. Brungs. (2007) Novel TiO2 thin film with non-UV activated super wetting and J. Mater. Chem.,17 952-958.

[10] M. Thelakkat, C. Schmitz, H. W. Schmidt (2002) Fully Vapor-Deposited Thin-Layer Titanium Dioxide Solar Cells Adv. Mater., 14 577. https://doi.org/10.1002/1521-4095(20020418)14:8<577.

[11] B. Peng, G. Jungmann, J. Claus. (2004) High-Performance TiO2 Photoanode with an Efficient Electron Transport Network for Dye-Sensitized Solar Cells *Coordin. Chem.Rev.*, 113 (36) 162.77–16282.

[12] P.T. Hsiao, Y.L. Tung, H.S. Teng. (2010) Structure and Electron-Conducting Ability of TiO2 Films from Electrophoretic Deposition and Paste-Coating for Dye-Sensitized Solar Cells. J. Phys. Chem. C, 115 (51), 25580–25589.

[13] M. Adachi, Y. Murata, I. Okada, S. Yoshikawa. (2003) Formation of Titania Nanotubes and Applications for Dye-Sensitized Solar Cells. J. Electrochem. Soc., 150 ~8! G488-G493 ~2003.
[14] Y. Suzuki, S. Ngamsinlapasathian, R. Yoshida, S. Yoshikawa. (2006) Partially nanowire-structured TiO2 electrode for dye-sensitized solar cellsCent. Eur. J. Chem. 4 (3), 476–488.
[15] C.J. Lin, W.Y. Yu, S.H. Chien. (2007) Effect of anodic powder as additive on electron transport properties in nanocrystalline dye-sensitized solar cells. Appl. Phys. Lett., 91 233120.
[16] S. Uchida, R. Chiba, M. Tomiha, N. Masaki, M. Shirai. (2002) Electronic structure of single-walled TiO2 and VO2 nanotubes Electrochemistry, 13, (1), 5-7.
[17] H. Yu, S.Q. Zhang, H.J. Zhao, G. Will, P.R. Liu; Electrochimica Acta, 54 (2009) 1319.
[18] S. Ito, T.N. Murakami, P. Comte, P. Liska, C. Grätzel, M.K. Nazeeruddin, M. Grätzel; Thin Solid Films, 516 (2008) 4613.
[19] J.B. Xia, N. Masaki, K.J. Jiang, S. Yanagida; Chem. Commun., 2 (2007) 138.
[20] Y.M. Liu, X.H. Sun, Q.D. Tai, H. Hu, B.L. Chen, N. Huang, B. Sebo, X.Z. Zhao; J. Pow. Soures, 196 (2011) 475.
[21] L. Kavan, B. O'Regan, A. Kay, M. Grätzel; J. Electroanal. Chem., 346 (1993) 291.
[22] R.S. Mane, C.D. Lokhande; Mater. Chem. Phys., 1 (2000) 65.
[23] J. Herrero, M.T. Gutierrez, C. Guillen, J.M. Dona, M.A. Martinez, A.M. Chapparo, R.Bayon; Thin Solid Films, 28 (2000) 361.
[24] P.K.Nair, M.T.S. Nair, A.Fernandez, M.Ocapo; J.Phys.D, 33 (1989) 829.
[25] C.D. Lokhande; Mater. Chem. Phys., 1 (1991) 27.
[26] K. Yokota, K. Nakamura, T. Sasakawa, T. Kamatani; Jpn J. Appl. Phys., 40 (2001)718
[27] A. D. Baker, D. Betteridge; Photoelectron Spectroscopy Appendix 2 (1972)
[28] G. M. Begun, C. E. Bamberger; Appl. Spectrosc. 43 (1989) 134.
[29] W Ma, Z. Lu, M. Zhang; Appl. Phys A, 66 (1998) 621.
[30] S. S. Amin, A. W. Nicholls, T. T. Xu; Nanotechnology, 18 (2007) 445609.
[31] F. Fabregat-Santiago, J. Bisquert, E. Palomares, L. Otero, D. Kuang, S. M. Zakeeruddin, M. Gratzel; The Journal of Physical Chemistry C, 111 (2007) 6550.
[32] Q. Wang, S. Ito, M. Graetzel, F. Fabregat-Santiago, I. Mora-Sero, J. Bisquert, T. Bessho, H. Imai; J. Phys. Chem. B, 110 (2006) 25210.
[33] Q. Wang, J.E. Moser, M. Gratzel; The Journal of Physical Chemistry B, 109 (2005)14945.
[34] V. Zwilling, M. Aucouturier, E. Darque-Ceretti; Electrochim. Acta, 45 (1999) 921.
[35] K. Zhu, N. Kopidakis, N. R. Neale, J. van de Lagemaat, A. J. Frank, J. Phys. Chem.B, 110, (2006) 25174.
[36] P. J. Cameron, L. M. Peter; J. Phys. Chem. B, 109 (2005) 7392.
[37] P. J. Cameron, L. M. Peter, S. Hore; J.Phys. Chem. B, 109 (2005) 930.
[38] A. Zaban, M. Greenshtein, J. Bisquert; Chem. Phys. Chem., 4 (2003) 859.